

# Planar Phased Array Calibration Based on Near-Field Measurement System

Rui Long\* and Jun Ouyang

**Abstract**—Matrix method for phased array calibration is an excitation reconstruction method by solving the linear equations based on the linear relationship between the measured near-field data and element excitations. In this paper, we propose a modified matrix method, in which the phased array model is simplified, to measure the element excitations of planar phased array. Our method reduces measurement time greatly at the cost of introducing some calibration errors. The introduced calibration errors can be minimized with the array excitation strategy proposed in this paper. Experimental results validate the effectiveness of our methods in calibrating planar phased arrays.

## 1. INTRODUCTION

PHASED array calibration, which is an important procedure of phased array engineering, ensures good performance of the array. The evaluation of the excitation of each radiating element is a fundamental part for calibrating phased array. Many calibration methods [1–7] need to use the phase shifters of a phased array, which causes that the phase shifters' performances influence the effectiveness of the methods greatly. To get rid of the restriction, the near-field measurement system is occupied in some calibration methods without the usage of phase shifters. Backward transformation method (BTM) and matrix method (MM) are the two major near-field calibration methods.

The BTM [8, 9] is also called microwave holographic metrology (MHM) [10]. It calculates the aperture field in front of the array with the measured planar near-field data based on the plane wave spectrum theory. The amplitude and phase of the aperture field in front of a radiating element are regarded as the excitation of the element. BTM has much lower calibration accuracy than MM because of the measured field truncation error, ignorance of evanescent plane waves and excitation extraction strategy.

The MM evaluates the element excitations by inverting the linear system relating the excitations to the measured data [11–14]. The linear system is represented with a set of linear equations. Let us consider (Fig. 1) a planar array consisting of  $N$  ( $N$  is the number of the array) radiating elements. A probe having effective height  $h(\theta, \phi)$  is placed in  $M$  ( $M$  is the number of measurement positions,  $M \geq N$ ) spatial points to measure the array near-field. The voltage at the probe output is expressed by the linear system

$$Ac = v \quad (1)$$

where  $c = (c_1, c_2, \dots, c_N) \in C^N$ .  $c_n$  is the excitation of the  $n$ -th element,  $n = 1, 2, \dots, N$ .  $v = (v_1, v_2, \dots, v_M) \in C^M$ .  $v_m$  is the probe voltage measured at point  $r'_m$ .  $r'_m$  is the position vector of the  $m$ -th measurement point,  $m = 1, 2, \dots, M$ .  $A \in C^{M \times N}$  is the coefficient matrix whose  $(m, n)$ -th element is equal to  $\exp(-j\beta r_{m,n}) / (4\pi r_{m,n}) f_n(\theta_{m,n}, \phi_{m,n}) \cdot h(\theta'_{m,n}, \phi'_{m,n})$ ,  $r_{m,n} = |r'_m - r_n| \beta$  is the wave

---

Received 20 November 2016, Accepted 30 December 2016, Scheduled 18 January 2017

\* Corresponding author: Rui Long (Longrui88@aliyun.com).

The authors are with the School of Electronic Engineering, University of Electronic Science and Technology of China (UESTC), Chengdu 611731, China.

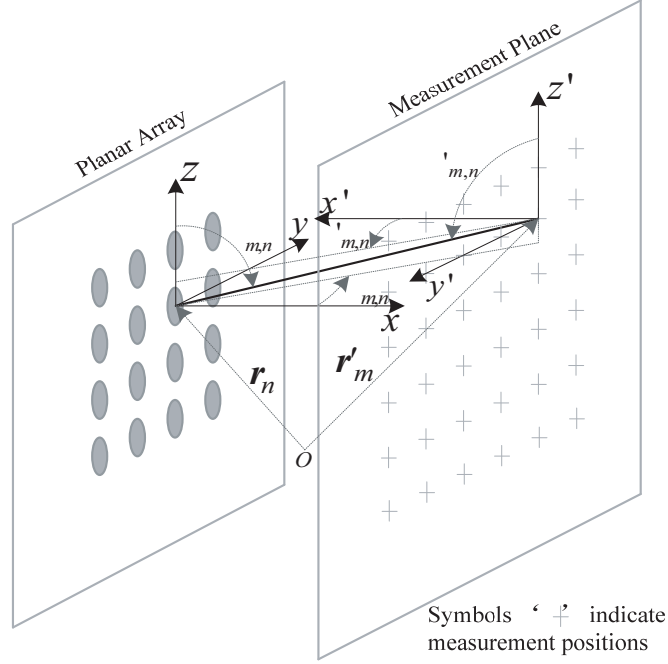


**Figure 1.** Illustration of the measurements in matrix method.

number.  $f_n(\theta, \phi)$  is the electric-field radiation pattern of the  $n$ -th radiating element.  $\theta_{m,n}$  and  $\phi_{m,n}$  are the relative vertical and horizontal angles between the  $m$ -th measurement point and  $n$ -th element position in a reference system centered on the  $n$ -th array radiating element.  $\theta'_{m,n}$  and  $\phi'_{m,n}$  are the relative vertical and horizontal angles between the  $n$ -th element position and  $m$ -th measurement point in a reference system centered on the  $m$ -th measurement point.

Solving linear equation (1) is evaluating the element excitations. The MM is suitable for both planar and conformal arrays [13]. However, the field at each measurement point radiated by each element is pre-measured to build matrix  $A$ , which is quite cumbersome especially for a large array.

In the case of a planar phased array, the MM is modified to reduce measurements and avoid the matrix ill-condition problem in this paper. The calibration errors of the MM are found to be related to the array excitation. Thus, the calibration errors can be reduced with a proper array excitation.

## 2. MODIFIED MATRIX METHOD

The  $n$ -th column of  $A$ , the mutual couplings between measurement probe placed at the measurement points and the  $n$ -th element, is associated with  $f_n(\theta, \phi)$ . For simplification, the radiation of each element is assumed to be an identical one,  $f(\theta_{m,n}, \phi_{m,n})$ , in the coordinate system centered on the element. For a planar phased array, the relative angles are correlated as in Eq. (2). In this case, the coefficient matrix  $A$  in Eq. (1) is modified to be  $\tilde{A}$ . The  $(m, n)$ -th element of  $\tilde{A}$  is as in Eq. (3).

$$\theta'_{m,n} = \pi - \theta_{m,n} \quad (2a)$$

$$\phi'_{m,n} = \phi_{m,n} \quad (2b)$$

$$a_{m,n} = \frac{\exp(-j\beta r_{m,n})}{4\pi r_{m,n}} \cdot f(\theta_{m,n}, \phi_{m,n}) \cdot h(\pi - \theta_{m,n}, \phi_{m,n}) \quad (3)$$

Since the array under calibration is planar and the measurement plane also planar, matrix  $\tilde{A}$  is determined by the relative angles between the measurement points and antenna positions. The measurement points are uniformly arranged and the relative positions of some measurement points are

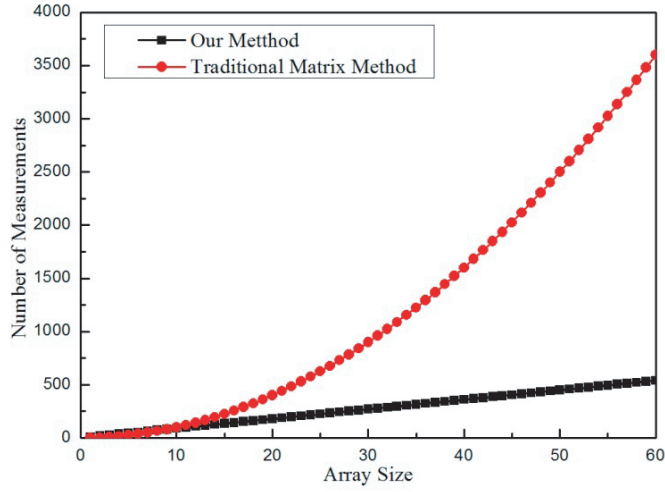


**Figure 2.** The comparison of the number of measurements.

the same as the relative positions of all the antenna elements. This strategy of picking measurement points makes  $\tilde{A}$  diagonally-dominant because the field attenuates from center to edge of the measurement plane. Besides, the number of measurements is greatly reduced compared with the traditional matrix method. As shown in Fig. 2, the number of measurements with our method is a linear function of the array size, and that of the tradition method is a 2nd order polynomial function of the array size. When the array size is large, our method needs much less calibration time.

Take a four-element one-dimensional uniform array for example as in Fig. 3, the measurement points are also arranged one-dimensionally.  $a_i$  is the coupling coefficient between an antenna element and the measurement probe in a measurement position, which is shown with a dotted arrow in Fig. 3.  $i$  is an integer indicating the relative position of the measurement probe and the antenna element. The matrix  $\tilde{A}$  in this example is similar to Toeplitz matrix as in Eq. (4), which means that the elements in the same diagonal of  $\tilde{A}$  are identical. If the antenna elements are not arranged uniformly,  $\tilde{A}$  is a sub-matrix formed with some columns of a diagonally-dominant Toeplitz matrix. Due to these properties, The matrix  $\tilde{A}$  in our modified MM usually has a relatively small condition number. As in Eq. (5), the linear system for calibration will not be ill-conditional.

$$\tilde{A} = \begin{pmatrix} \bullet & \bullet & \bullet & \bullet \\ a_{-1} & a_{-2} & a_{-3} & a_{-4} \\ a_0 & a_{-1} & a_{-2} & a_{-3} \\ a_1 & a_0 & a_{-1} & a_{-2} \\ a_2 & a_1 & a_0 & a_{-1} \\ \bullet & \bullet & \bullet & \bullet \end{pmatrix} \tag{4}$$

$$\tilde{A}\tilde{c} = v \tag{5}$$

$\tilde{c}$  is the calculated array excitation with our modified MM. The difference between  $c$  in Eq. (1) and  $\tilde{c}$  in Eq. (5) is the calibration error caused by the simplification, which is defined as in Eq. (6).  $c$  is the true array excitation, and it is also the calculated vector with the traditional MM method without any errors. Based on Eqs. (1) and (5), the calibration errors are evaluated as in Eq. (7).  $\tilde{A}^+$  is the Moore-Penrose pseudo-inverse of  $\tilde{A}$ .

$$\Delta c = \tilde{c} - c \tag{6}$$

$$\Delta c = \tilde{A}^+ (A - \tilde{A}) c \tag{7}$$

$\Delta c$  is largely related to  $c$ . To study the effect of the true array excitation  $c$  on the calibration errors  $\Delta c$ , singular value decomposition is applied to the matrix  $\tilde{A}^+(A - \tilde{A})$  during the norm evaluation of  $\Delta c$

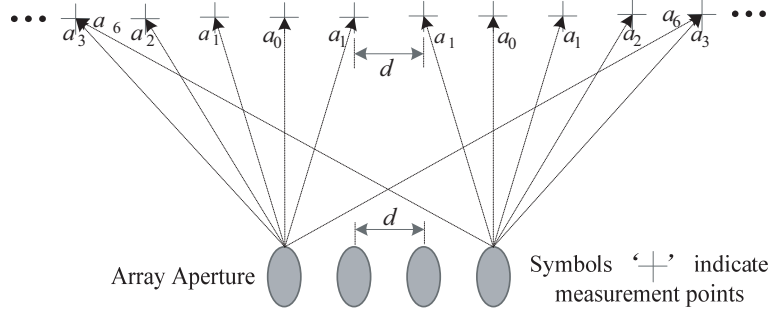


**Figure 3.** Illustration of the couplings between the measurement probe in the measurement points and the antenna elements.

as in (8).  $\sigma_i$  is a singular value of  $\tilde{A}^+(A - \tilde{A})$ .  $U$  and  $V$  are unitary matrices. Calibration accuracy is expressed as the relative value of  $\Delta c$  and  $c$  as in Eq. (9). If  $t_i = 0$ ,  $i \neq N$ ,  $\|\Delta c\|_2/\|c\|_2$  gets its minimum value  $\sigma_N$ . If  $t_i = 0$ ,  $i \neq 1$ ,  $\|\Delta c\|_2/\|c\|_2$  gets its maximum value  $\sigma_1$ .

$$\|\Delta c\|_2 = \left\| \tilde{A}^+ (A - \tilde{A}) c \right\|_2 = \|UDVc\|_2 = \|DVc\|_2 = \left\| (\sigma_1 t_1, \sigma_2 t_2, \dots, \sigma_N t_N)^T \right\|_2 = \sqrt{\sum_{i=1}^N |\sigma_i t_i|^2} \quad (8a)$$

$$D = \text{diag}(\sigma_1, \sigma_2, \dots, \sigma_N), \sigma_1 \geq \sigma_2 \geq \dots \geq \sigma_N \geq 0 \quad (8b)$$

$$Vc = (t_1, t_2, \dots, t_N)^T \quad (8c)$$

Given the true array excitation, the calibration accuracy is evaluated as in Eq. (9). The best calibration accuracy is realized when the true array excitation satisfies Equation (10a). The worst calibration accuracy happens when the true array excitation satisfies Equation (10b). As a result, the best array excitation during calibration is the last column of matrix  $V^H$  because  $V$  is a unitary matrix.

$$\frac{\|\Delta c\|_2}{\|c\|_2} = \frac{\|\Delta c\|_2}{\|Vc\|_2} = \sqrt{\sum_{i=1}^N |\sigma_i t_i|^2} / \sqrt{\sum_{i=1}^N |t_i|^2} \quad (9)$$

$$Vc_{\text{best}} = (0, 0, \dots, 1)^T \quad (10a)$$

$$Vc_{\text{worst}} = (1, 0, \dots, 0)^T \quad (10b)$$

According to the above analysis, the determination of the best array excitation is based on knowing  $A$ , which has been modified to be  $\tilde{A}$  in the proposed method. As an alternative, the simulated data can be used to do this. With the simulation model of the array and measurement probe, the simulated active antenna element near-fields are obtained. Thus, a wanted array excitation used to realize calibration accuracy as high as possible is calculated.

Even we know that the true array excitation has effect on calibration accuracy, we cannot implement the wanted actual array excitation because there is excitation error which needs to be calibrated exactly. Thus, the iterative calibration method is used. Two or three more array near-fields are measured. For example, after the first array near-field measurement procedure, we calculate the excitation error and excite the array uniformly taking the error into account. Then, we measure the array near-field again and calculate the excitation error again. If the difference between the last calculated excitation error and the last but one calculated excitation error is less than a threshold such as 10%, the average error of them is considered as the array excitation error under uniform array excitation, and this calibration procedure stops. Otherwise, we excite the array uniformly again, measure the array near-field again, calculate the excitation error again and estimate the convergence again. Iterative calibration method can also be implemented under other array excitations. In the practical engineering, we can calibrate a phased array under several array excitations and pick the best one.

### 3. EXPERIMENT

In this section, an eight-element L-band microstrip antenna array is constructed for measurement. The NSI near-field measurement system is used. Fig. 4 shows photos of the experiment system and the power divider and phase shifters used. The proposed experiment system comprises: 1) a wooden support which has little effect on the antenna performance; 2) an eight-way Wilkinson power divider; 3) coaxial cables with different lengths to implement the four phase delays of  $0^\circ$ ,  $90^\circ$ ,  $180^\circ$  and  $270^\circ$  at 2-GHz; 4) an eight-element microstrip antenna array at the resonant frequency of 2-GHz with 75 mm element spacing; 5) open-ended waveguide as the measurement probe. During the experimental study, the sinusoidal signal of 2 GHz generated by the vector network analyzer is equally divided into eight parts by the Wilkinson power divider. Different phase delays of the eight-way signals are realized with the coaxial cables shown in Fig. 4(c). The delayed eight-way signals are radiated by the eight-element microstrip antenna array. The output signal of the open-ended waveguide is measured by the vector network analyzer.

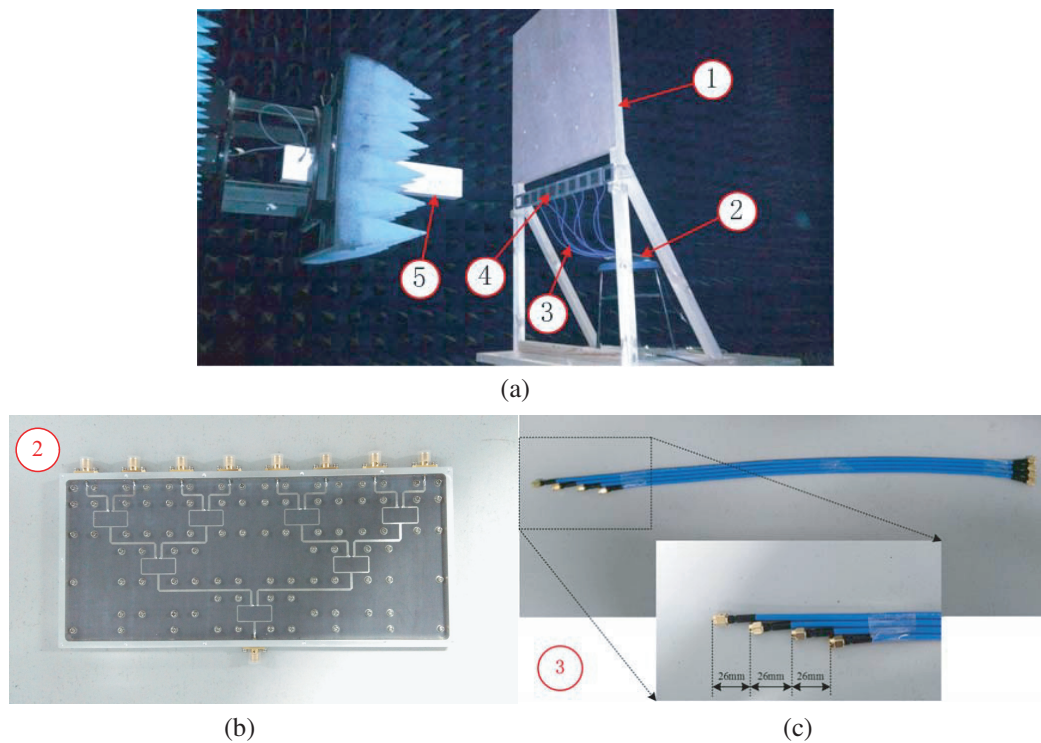


**Figure 4.** Photos of the experiment system: (a) overview; (b) power divider; (c) coaxial cables with four different phase delays of  $0^\circ$ ,  $90^\circ$ ,  $180^\circ$  and  $270^\circ$ .

The details of the experimental procedure are shown as follows.

- 1) The simulation model of the experiment system is constructed to calculate the near-fields of antenna elements. With the simulated near-fields, the best and worst array excitations for this calibration experiment are calculated. They are amplitude-uniform because only an eight-way Wilkinson power divider is used to control array excitation amplitude. The phase of each element excitation is one of the four phase delays of  $0^\circ$ ,  $90^\circ$ ,  $180^\circ$  and  $270^\circ$ . Three array excitation cases are listed in Table 1. Case 1 is the best. Case 2 is the worst. Case 3 is that the array excitation is equiphase. This step is implemented before the near-field measurement system is occupied.
- 2) The near-field of the fourth element of the array, whose elements are numbered from left to right, in Fig. 4(a) is measured. As the array is one-dimensional, only the near-field on a line is necessary. The line is 500 millimeters away from the array and 6 meters long. The array is parallel to the

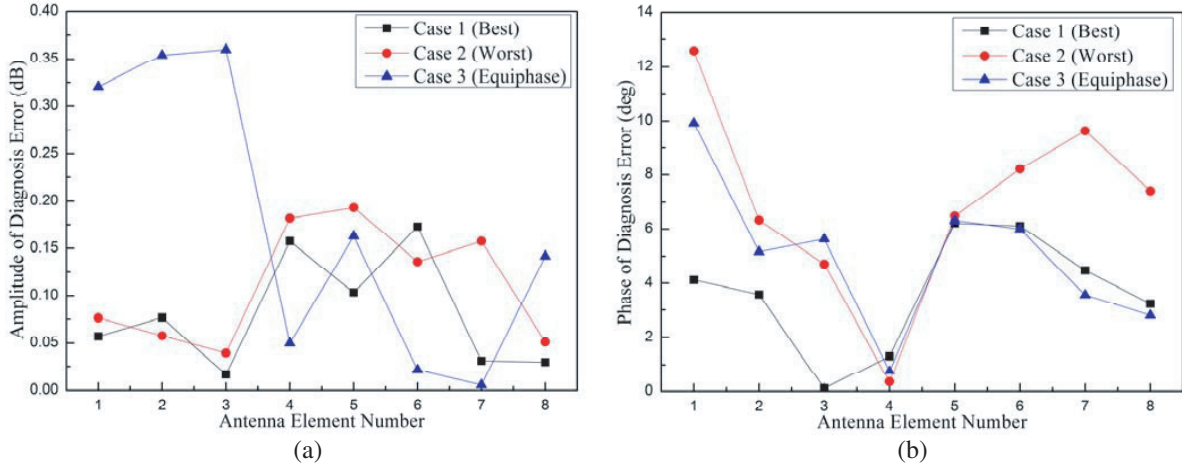
**Table 1.** Array excitation phases for the calibration example.

Antenna number	1	2	3	4	5	6	7	8
Case 1 (best)	270	0	180	0	0	90	270	0
Case 2 (worst)	270	180	90	0	180	180	90	0
Case 3	0	0	0	0	0	0	0	0

line. The measurement point spacing is 75 millimeters, which is also the antenna element spacing. Then, three near-fields of the array when the array excitation phase is the three cases in Table 1 are also measured. When the antenna element near-field is being measured, the other elements are matched.

- 3) The coefficient matrix  $\tilde{A}$  in Eq. (5) is created with the measured element near-field. It is well-conditioned with a condition number of 1.465. Three array excitations are calculated for the three cases with our modified MM. Calibration errors are the differences between the calculated array excitations and true array excitations, which are amplitude-uniform and the phases in Table 1.

Calibration errors for the three cases are shown in Fig. 5. The average amplitude and phase error in Case 1 are 0.0807 dB and 3.6435 degrees, respectively. The average amplitude and phase error in Case 2 are 0.1116 dB and 6.9651 degrees, respectively. The average amplitude and phase error in Case 3 are 0.1770 dB and 5.0187 degrees, respectively. Case 1 has the minimum calibration errors in both amplitude and phase as predicted. Case 3 has larger amplitude errors and smaller phase errors than Case 2. Thus, it is necessary to calculate the calibration accuracy  $\|\Delta c\|_2/\|c\|_2$  as in Eq. (9). The calibration accuracy results are listed in Table 2. Case 1 has the highest accuracy, and Case 2 has the lowest one as predicted.

**Figure 5.** Array calibration errors under the three array excitation phases.**Table 2.** Calibration accuracy results for the calibration example.

Diagnosis Accuracy	Case 1 (Best)	Case 2 (Worst)	Case 3 (Equiphase)
$\ \Delta c\ _2/\ c\ _2$	2.69%	4.81%	3.82%

The experimental results validate the effectiveness of our modified MM for planar phased array calibration and the influence of the array excitation on the calibration accuracy.

#### 4. CONCLUSION

This paper proposes a modified MM for planar phased array calibration with a planar near-field measurement system. Compared with the traditional MM, our method has much lower complexities of measurements and data processing especially for large scale arrays. However, for conformal phased array calibration, the traditional MM is better. How the array excitation influences the calibration accuracy of MM is first analyzed in this paper. According to the analysis, the calibration accuracy can be improved with the array excitation optimization. Experimental results validate the modified MM and the effect of array excitation on calibration accuracy.

#### REFERENCES

1. Mano, S. and T. Katagi, "A method for measuring amplitude and phase of each radiating element of a phased array antenna," *Electronic and Communication in Japan*, Vol. 65-B, No. 5, 1982.
2. Sorace, R., "Phased array calibration," *IEEE Trans. Antennas Propag.*, Vol. 49, No. 4, 517–525, Apr. 2001.
3. Takahashi, T., Y. Konishi, S. Makino, H. Ohmine, and H. Nakaguro, "Fast measurement technique for phased array calibration," *IEEE Trans. Antennas Propag.*, Vol. 56, No. 7, 1888–1899, Jul. 2008.
4. Silverstein, S. D., "Application of orthogonal codes to the calibration of active phased array antennas for communication satellites," *IEEE Trans. Antennas Propag.*, Vol. 45, No. 1, 206–218, Jun. 1997.
5. Lee, K. M., R. S. Chu, and S. C. Liu, "A built-in performance-monitoring/fault isolation and correction (PM/FIC) system for active phased-array antennas," *IEEE Trans. Antennas Propag.*, Vol. 41, No. 11, 1530–1540, Nov. 1993.
6. Keizer, W. P. M. N., "Fast and accurate array calibration using a synthetic array approach," *IEEE Trans. Antennas Propag.*, Vol. 59, No. 11, 4115–4122, Nov. 2011.
7. He, C., X. L. Liang, J. P. Geng, and R. H. Jin, "Parallel calibration method for phased array with harmonic characteristic analysis," *IEEE Trans. Antennas Propag.*, Vol. 62, No. 1, 5029–5036, Oct. 2014.
8. Hanfling, J. D., G. Borgiotti, and L. Kaplan, "The backward transform of the near field for reconstruction of aperture fields," *IEEE Antennas and Propagation Society International Symposium*, Vol. 17, 764–767, 1979.
9. Lee, J. J., E. M. Ferren, D. P. Woollen, and K. M. Lee, "Near-field probe used as a diagnostic tool to locate defective elements in an array antenna," *IEEE Trans. Antennas Propag.*, 884–889, 1988.
10. Logan, J. T., D. S. Reinhard, and K. E. Hauck, "Phased array calibration and diagnostics utilizing a student-built planar near-field system," *2010 IEEE International Symposium on Phased Array Systems and Technology (ARRAY)*, 279–286, 2010.
11. Gattoufi, L., D. Picard, A. Rekiouak, and J.-C. Bolomey, "Matrix method for near-field diagnostic techniques of phased arrays," *IEEE International Symposium on Phased Array Systems and Technology*, 52–57, 1996.
12. Migliore, M. D. and G. Panariello, "A comparison of interferometric methods applied to array diagnosis from near-field data," *IEE Proceedings, Microwaves, Antennas and Propagation*, Vol. 148, No. 4, 261–267, 2001.
13. Bucci, O. M., D. Migliore, G. Panariello, and P. Sgambato, "Accurate diagnosis of conformal arrays from near-field data using the matrix method," *IEEE Trans. Antennas Propag.*, Vol. 53, No. 3, 1114–1120, Mar. 2005.
14. Migliore, D., "A compressed sensing approach for array diagnosis from a small set of near-field measurements," *IEEE Trans. Antennas Propag.*, Vol. 59, No. 6, 2127–2133, Jun. 2011.